ChemComm

This article can be cited before page numbers have been issued, to do this please use: C. Huang, J. Wu, C. Song, R. Ding, Y. Qiao, H. Hou, J. Chang and Y. Fan, *Chem. Commun.*, 2015, DOI: 10.1039/C5CC02432C.

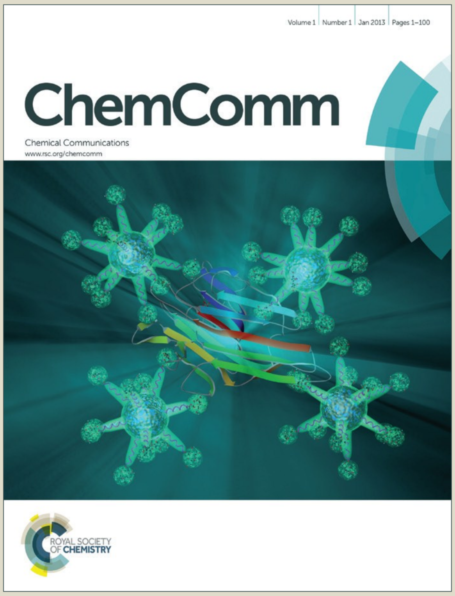

ROYAL SOCIETY OF CHEMISTRY

www.rsc.org/chemcomm

View Article Online
DOI: 10.1039/C5CC02432C

Journal Name

COMMUNICATION

Received 00th January 20xx,
Accepted 00th January 20xx

DOI: 10.1039/x0xx00000x

www.rsc.org/

Reversible Conversion of Valence-Tautomeric Copper Metal-Organic Frameworks Dependent Single-Crystal-to-Single-Crystal Oxidation/Reduction: Redox-Switchable Catalyst for C–H Bonds Activation Reaction

Chao Huang, Jie Wu*, Chuanjun Song, Ran Ding, Yan Qiao, Hongwei Hou*, Junbiao Chang* and Yaoting Fan

Upon single-crystal-to-single-crystal (SCSC) oxidation/reduction, reversible structural transformations took place between the anionic porous zeolite-like Cu^I framework and a topologically equivalent neutral Cu^ICu^{II} mixed-valent framework. The unique conversion behavior of the Cu^I framework endowed it as redox-switchable catalyst for direct arylation of heterocycle C–H bonds.

The redox-active metal-organic frameworks (*ra*-MOFs),[1] derived from direct incorporation of redox active competent building blocks into the MOFs have been attracting much attention as the more possible candidates for a new class of multifunctional hybrid materials, such as, electrode materials,[2] electrical conductors,[3] selective gas adsorption,[4] catalysts,[5] ferroelectric and ferromagneticmaterials,[6] etc. In *ra*-MOFs, an exciting yet little explored area is that a few *ra*-MOFs could proceed single-crystal-to-single-crystal (SCSC) structural transformations, including central metal valence tautomerism and reassembly of metal-ligand connectivity and network topology, caused by redox reagents[7] or mechanochemistry.[8] During the transformations, their capacity of altering the oxidation valence states of metal centers, skeleton structure, and framework charge rewards them peculiar physical and chemical applications, such as switchable catalyst,[7a] ion exchange, and reducing agents for the synthesis of monodispersed metal nanoparticles.[7f-g] Besides, so far, a handful of positive-charged Cu^I MOFs incorporating free counteranions in the channels or pores have shown fascinating host-guest dependent SCSC structural transformation to Cu^{II} MOFs driven by oxidation reactions.[9] These examples indicated that it should be practicable to tune the SCSC redox processes through host-guest interactions. Notably, the reversible SCSC transformation of *ra*-MOFs are more eagerly anticipated for the advancement of switching and sensing materials, yet only a single example of reversible SCSC reduction/reoxidation behaviour of Ru^{III}/Ru^{II} chiral MOFs was presented by Lin.[7a]

Considering the potential applications in switchable catalysts and sensors of porous Cu^I MOFs with tunable SCSC structural transformation, chemists are keen to design and synthesize redox-convertible Cu^I MOF materials capable of reversible SCSC structural conversions relying on the host-guest chemistry. Although a few Cu^I MOFs oxidized to Cu^{II} MOFs through a SCSC process have been presented,[7e, 9] the intricate mechanism involved in these central metal valence tautomerism in a SCSC fashion remains largely unclear and attempts to oxidize Cu^I MOFs with oxidants (O_2, H_2O_2, I_2, etc.) always lead to the MOFs dissolving or crystallinity loss. Even harder, the reduction of Cu^{II} in the framework through a SCSC fashion is still very challenging and has never been observed, not to mention the reversible SCSC oxidation/reduction structural transformations between them.

Herein, we report the assembly of a Cu^I complex $\{(H_3O)[Cu^I_2(CN)(TTB)_{0.5}]\cdot1.5H_2O\}_n$ (**1**) (H_4TTB = 1,2,4,5-tetra(1H-tetrazole-5-yl)-benzene) with an anionic, porous zeolite-like three-dimensional (3D) framework containing free $[H_3O]^+$ ions as guest molecules. Upon SCSC oxidation/reduction, interesting reversible structural transformations took place between the anionic Cu^I framework of **1** and a topologically equivalent neutral Cu^ICu^{II} mixed-valent framework of $\{[Cu^ICu^{II}(CN)(TTB)_{0.5}]\cdot1.5H_2O\}_n$ (**2**). A mechanism for the reversible transformations was proposed, which indicated that **1** and **2** showed the first example of host-guest dependent reversible SCSC oxidation/reduction behavior of Cu^I/Cu^ICu^{II} MOFs. In addition, we developed **1** into an effective heterogeneous catalyst for the direct C–H bond arylation of heteroarenes, while its oxidized transformer **2** as catalyst under identical conditions led mainly to the formation of Ullmann coupling products.

Imitating the preparation of some charged small pore zeolites, especially those presenting free counteranions in the channels of their structure, the introduction of organic structure directing agents (OSDAs) into the hybrid inorganic-organic matrix have been applied.[10] Reaction of CuCN with H_4TTB in dimethylformamide (DMF)/EtOH/$NH_3\cdot H_2O$ at 160 °C for 3 days with N,N-diisopropylethylamine (DIPEA) as OSDA afforded primrose yellow

---

The College of Chemistry and Molecular Engineering, Zhengzhou University, Zhengzhou, Henan, 450001, P. R. China
Email: wujie@zzu.edu.cn houhongw@zzu.edu.cn changjunbiao@zzu.edu.cn

† Electronic Supplementary Information (ESI) available: Experimental information; theoretical calculations; characterization data for all compounds, including figures for ORTEP, XPS, XRPD, TG, CIF files and crystal data. CCDC reference numbers: 1041835-1041839 for **1**, **1a**, **2-4**. See DOI: 10.1039/x0xx00000x

View Article Online
DOI: 10.1039/C5CC02432C

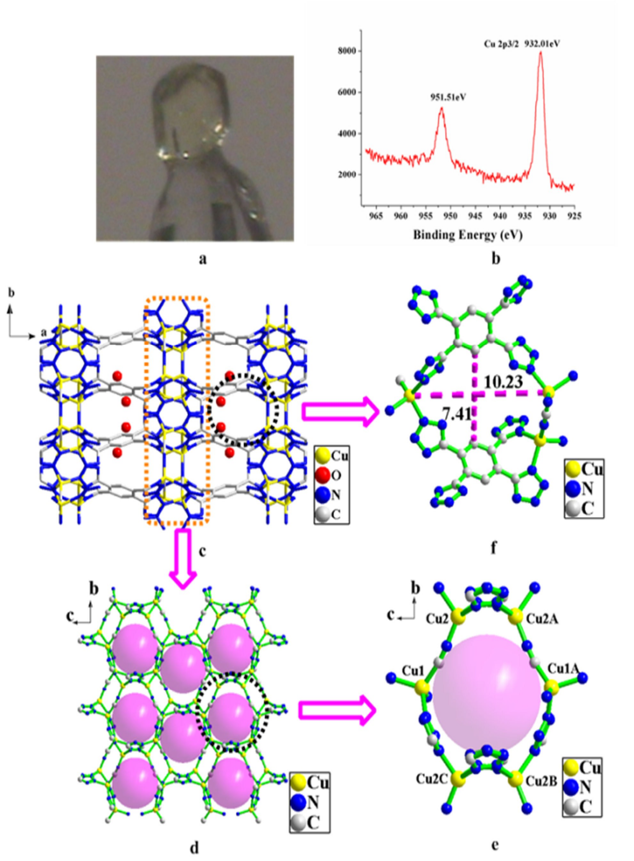

Figure 1. Crystal structure of **1**: (a) Photograph showing the primrose yellow single crystal of **1**. (b) XPS spectrum of **1**. (c) View of the 3D network of **1** along *c* axis. (Oxygen atoms represented as $[H_3O]^+$ ions). Hydrogen atoms and free water molecule are omitted for clarity. (d) The 2D layer along *a* axis. (e) Each layer was composed of two cyano groups, six tetrazole rings, and six Cu^I cations. (f) The dimension of the channel with 10.23 × 7.41 Å at the *ab* plane.

single crystals. Single-crystal X-ray diffraction analysis revealed that $\{(H_3O)[Cu^I_2(CN)(TTB)_{0.5}]\cdot 1.5H_2O\}_n$ (**1**) shows a monoclinic C2/c space group and an anionic, porous zeolite-like 3D framework with free $[H_3O]^+$ ions encapsulated inside the cavity (Figure 1). The univalent copper centers in **1** were revealed by primrose yellow product and supported by X-ray photoelectron spectroscopy (XPS).[9a, 11]

PLATON analysis gave the free void volume ratio of 54.8% in **1**, which suggests a microporous characteristic of **1**. As shown in Figure 1d, Cu^I cations are linked through cyano groups and tetrazole rings to form a 2D layer containing open cavities with a maximum inner width of ~7.0 Å (considering van der Waals radii) along *a* axis (Figures 1d and e). Such layers are further connected by TTB^{4-} groups, leading to the formation of a 3D zeolite structure with dimensions of the channels being 10.23 × 7.41 Å along *c* axis (Figure 1f). The asymmetric unit of **1** contains half of deprotonated TTB^{4-} anion, two Cu^I ions, and one cyano anion (Figure S1a). Overall, the framework of **1** is anionic and is filled with $[H_3O]^+$ ions and guest water molecules. Given the charge-balance consideration, there should be one $[H_3O]^+$ ion per formula unit.

Experimentation aimed at evaluating the redox properties of **1** showed that a reversible oxidation/reduction transformation could be achieved. When the single crystal samples of **1** were left open to air at ambient temperature for more than three days, slow conversion into an oxidized complex with retention of single crystallinity occurred. This could be easily validated by observation that the primrose yellow crystals gradually turned into black (Figure 2a), and further verified by XPS (Figure 2b).[9a, 11] XPS and variable temperature magnetization measurements on the black samples supported the change from Cu^I complex **1** to a mixed-valent Cu^ICu^{II} complex (Figure S3b). When the primrose yellow single crystals of **1** were heated at 60, 80, and 100 °C, they turned to black within 25, 12, and 5 min, respectively. Conversion was sufficiently complete inside and outside within 12 h at 100 °C. Remarkably, the crystal remained intact throughout this transformation, enabling the structure of the black crystal samples to be determined.

Single-crystal X-ray analysis of the black single crystal revealed a new crystallographic form $\{[Cu^ICu^{II}(CN)(TTB)_{0.5}]\cdot 1.5H_2O\}_n$ (**2**) (Figure 2c). The conversion from **1** to **2** implies a slightly increase of 0.0[illegible] Å of *a* axis, 0.03 Å of *c* axis, and is accompanied by an increase of more than 1.1° of *β* angle (Table S1). Further studies showed that the metal-ligand connectivity and network topology of **2** are consistent with that of **1** though some of their corresponding bond lengths and angles are different (Table S2).

Theoretical calculations presented the charges on Cu1 and Cu2 being 0.631 and 0.052 *e*, respectively, which indicated that Cu1 is oxidized (Figure 2d). Due to half of Cu^I ions in **1** being oxidized to Cu^{II} ions, the framework of **2** becomes neutral. The oxidation framework transformation from **1** to **2** with metal-ligand connectivity and network topology unchanged was crosschecked by

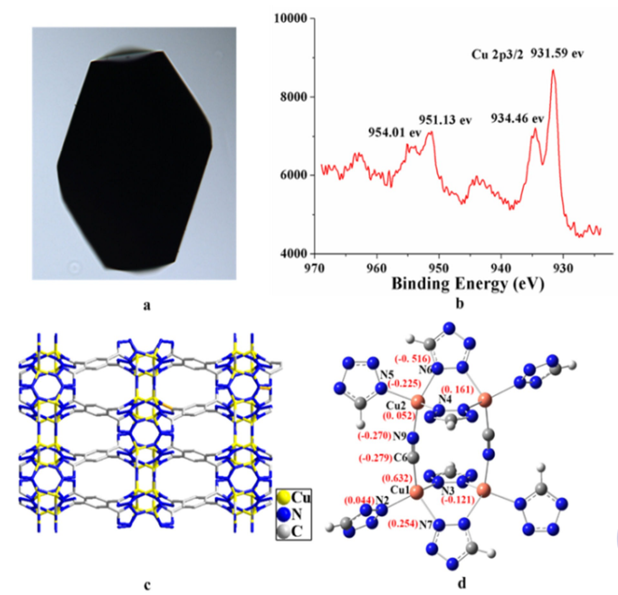

Figure 2. Crystal structure of **2**: (a) Photograph showing the black single crystal of **2**. (b) XPS spectrum of **2**. (c) View of the 3D network of **2** down *c* axis. Hydrogen atoms and free water molecule are omitted for clarity. (d) Optimized structure of **2** with UB3LYP functional and 6-31+G* basis set for C, H, N and 6-311++G** basis set for Cu. Values in parentheses are the calculated mulliken charges for selected atoms.

View Article Online
DOI: 10.1039/C5CC02432C

the identical powder X-ray diffraction (PXRD) peaks of **2** compared to those of **1** (Figure S3d). Besides, in the variable-temperature power X-ray diffraction (VTPXRD; see Figure S2b) patterns of **1**, the main diffraction peaks remained unchanged at the temperature ranging from 25 to 275 °C, though in the high temperature range (i.e. 100~275 °C) the color of samples turned into black and the Cu^I framework was oxidized into Cu^ICu^{II} framework identified by XPS.

Notably, the transformation from Cu^I complex into Cu^ICu^{II} mixed-valent complex is reversible. Treatment of the single crystal samples of **2** with reducing agent (ascorbic acid) led to a color change from black to primrose yellow, thus suggesting the reduction of Cu^ICu^{II} centers to Cu^I centers in the MOFs. The result was further confirmed by XPS of the reduced samples. Interestingly, the reduction of **2** also took place in a SCSC fashion. Single-crystal X-ray structure studies on the reduced sample $\{(H_3O)[Cu^I_2(CN)(TTB)_{0.5}]\cdot 2H_2O\}_n$ (**1a**) indicated that its framework is essentially identical to that of **1** but with different amounts of lattice H_2O. The free $[H_3O]^+$ ions in **1a** could be provided by the ascorbic acid. PXRD further indicated that **1a** retained the single-crystal nature and closely matched that of **1** but with different degrees of crystallinity.

The primrose yellow reduced crystals of Cu^I complex **1a** could be reoxidized in air to afford black crystals of Cu^ICu^{II} mixed-valent complex **2a** in a SCSC fashion, which was further supported by the XPS and X-ray analysis (Figure S5). PXRD and unit-cell determinations indicated that **2a** remained single crystals with the same structure as **2**. The transformations between Cu^I complexes (**1** and **1a**) and Cu^ICu^{II} mixed-valent complexes (**2** and **2a**) in this work showed totally reversible SCSC reduction/oxidation processes.

Further studies indicated that the anionic framework of **1** displays distinct redox behavior depending on the nature of the guests. With triethylamine (TEA) and diisopropylamine (DIPA) as OSDAs, Cu^I complexes $\{(TEAH)[Cu^I_2(CN)(TTB)_{0.5}]\cdot H_2O\}_n$ (**3**) and $\{(DIPAH)[Cu^I_2(CN)(TTB)_{0.5}]\cdot 0.5H_2O\}_n$ (**4**) with the same anionic framework as that of **1** were obtained, respectively, which became redox inert (Figures S6 and S7).

Complex **1** could be an ideal Cu^I MOF-based structural model for application in redox-convertible heterogeneous catalysis with C–H activation due to the following considerations: (i) the construction of porous Cu^I-MOF **1** may provide a convenient heterogeneous self-support catalyst with Cu^I ions acting as both metal nodes and catalytic sites for the C–H bond activation reaction; (ii) importantly, the totally reversible SCSC oxidation/reduction behaviors of **1** and **2** make them perfectly capable as redox-convertible catalysts. Herein, **1** and **2** were employed in the direct C–H bond arylation of heteroarenes.

The optimization of the reaction conditions for **1**-catalyzed C–H arylation reaction was performed using benzothiazole and iodobenzene as coupling partners. As shown in Scheme S1, after extensive screening of solvents, temperature and bases, the standard conditions were obtained using two equivalent of K_2CO_3 as the base in the presence of 2.5 mol % of crystal samples of **1** in DMF at 140 °C for 10 h, giving the desired arylation product in 90% yield. To ensure that the reaction catalyzed by **1** took place predominantly within the crystal voids rather than on the external surface, the C–H arylation reaction was performed with crystals of **1** (~0.3 × 0.3 × 0.2 mm^3). It eliminated the possibility of catalytic activity resulting from the surface metal sites of very tiny particles because big crystals own too few surface metal sites to account for the catalytic reaction. Remarkably, **1** could maintain the crystallinity after the catalytic reaction. Single-crystal X-ray analysis and XPS of the single crystal samples after reaction revealed the identical framework as that of **1**. Inductively coupled plasma atomic emission spectrometry (ICP) analysis of the filtrate showed that less than 0.1% of the copper was leached into solution after 10 hours under the typical reaction conditions, strongly confirming its heterogeneity. In the recyclability experiments, **1** was readily recovered from the catalytic reaction via centrifugation, and the recovered catalyst showed only slight deterioration after five runs. Moreover, the PXRD patterns of the **1** crystallites after the fifth catalytic reaction closely matched those of single crystals of **1** and showed no signs of framework collapse and decomposition, which indicated that the framework could remain intact after at least five runs(Figure S9).

Subsequently, this new catalytic system was found to be general for the coupling of heteroarenes with a variety of substituted aryl or heteroaryl halides, and the results were summarized in Table . Compared with the homogeneous CuI systems, the coupling of substrates with catalyst **1** required longer reaction times arising from the slow diffusion of substrates and products through the MOF channels. However, the catalytic system with recyclable catalyst **1** in the presence of mild inorganic base not only met the preference of modern green chemistry for more environmentally friendly conditions, but also improved tolerance of functional groups and thereby extending the scope of possible substrates. The high efficiency of the current **1** system is believed to stem from its unique structural features and redox behavior. The porous zeolite-like framework of **1** has microporous characteristic with a large free volume and channels along *a* and *c* axes, which can facilitate the transport organic substrates and products. In addition, we rationalized that the potential redox activity of **1** is crucial for C–H activation, especially for the oxidative addition step. The catalytic reaction is assumed to perform through the base assisted formation of heteroarylcopper species formed by the reacting atoms of deprotonated heterocycles superimposed on the active Cu^I centers of the catalyst, and subsequent reaction of this species with aryl halide. The framework of **1** with isolated catalytically active sites could stabilize the highly active heteroarylcopper species, preventing any intermolecular deactivation pathways and facilitate the halide displacement step.

We then tested the coupling reaction of iodobenzene or *p*-iodoanisole with heteroarenes using crystal samples of **2** instead of

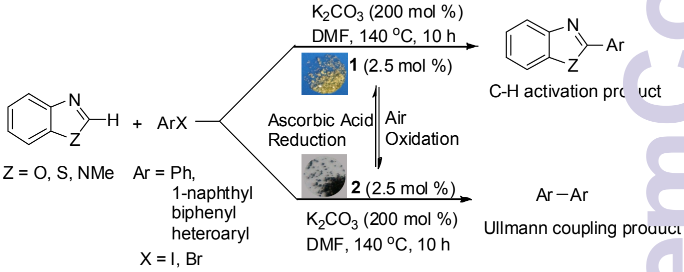

Scheme 1. Schematic view of redox-convertible catalysts **1** and **2** for the direct C–H bond arylation of heteroarenes.

View Article Online
DOI: 10.1039/C5CC02432C

1 as catalyst under identical conditions (Scheme 1). Interestingly, it was found that the reactions gave the Ullmann coupling product as the major product (> 70%), together with a small amount of the C–H activation product (< 10%). The Cu^ICu^{II} mixed-valent complex **2** mainly catalyzed the Ullmann coupling reactions because the $[Cu^I_2Cu^{II}_2(CN)_2]^{4+}$ unit in **2** could be regarded as an active species and enhance the rate of the Ullmann coupling reaction.[12] The coupling product was thus formed by oxidative addition of **2** to the aryl iodide followed by reductive elimination. **2** also could be recycled and reused at least five times without significant loss of catalytic activity and MOF crystallinity (Figure S10).

Therefore, **1** can use as a redox-convertible catalyst for C–H activation. For the coupling of heteroarenes with aryl and heteroaryl halides, catalytically active Cu^I-based catalyst **1** can be transformed through SCSC oxidation process to Cu^ICu^{II}-based **2**, which could selectively catalyze the Ullmann coupling reaction. Conversely, the reduction of **2** turns on the catalytic activity for the direct C–H bond arylation of heteroarenes, and the resulting Cu^I-based catalyst **1** is highly active.

In conclusion, we report the first observation of an interesting anionic porous zeolite-like Cu^I complex **1** (primrose yellow) capable of reversible structural transformation to a topologically equivalent neutral Cu^ICu^{II} mixed-valent complex **2** (black) upon SCSC oxidation/reduction. The reversible SCSC redox behavior of **1** can be ascribed to the host-guest interactions during the redox processes and its intrinsic features, such as the flexibility of the framework to allow the deformation and the strong ability of the multinuclear Cu^I units to capture O_2 molecules. In addition, for the coupling of heteroarenes with aryl and heteroaryl halides, C–H bond activation products and Ullmann coupling products were obtained, respectively, with **1** and **2** as catalyst. Therefore, the unique structural features and redox behavior of **1** endow it with versatile characteristics as heterogeneous catalyst such as high catalytic activity, recyclability for reuse, and redox-convertible catalyst for the C–H bond activation reaction.

We are grateful for financial support from the National Natural Science Foundation of China (Nos. 21201152, 81330075, and 21371155) and Research Found for the Doctoral Program of Higher Education of China (20124101110002).

Notes and references

1 (a) H. Miyasaka, *Acc. Chem. Res.*, 2013, **46**, 248-257; (b) J. Jelic, D. Denysenko, D. Volkmer and K. Reuter, *New. J. Phys.*, 2013, **15**, 11504; (c) C. Remenyi and M. Kaupp, *J. Am. Chem. Soc.*, 2005, **127**, 11399-11413.

2 (a) M. Okubo, D. Asakura, Y. Mizuno, J. D. Kim, T. Mizokawa, T. Kudo and I. Honma, *J. Phys. Chem. Lett.*, 2010, **1**, 2063-2071; (b) M. Nagarathinam, K. Saravanan, E. J. H. Phua, M. V. Reddy, B. V. R. Chowdari and J. J. Vittal, *Angew. Chem., Int. Ed.*, 2012, **51**, 5866-5870.

3 (a) A. A. Talin, A. Centrone, A. C. Ford, M. E. Foster, V. Stavila, P. Haney, R. A. Kinney, V. Szalai, F. E. Gabaly, H. P. Yoon, F. Léonard and M. D. Allendorf, *Science*, 2014, **343**, 66-69; (b) Y. Kobayashi, B. Jacobs, M. D. Allendorf and J. R. Long, *Chem. Mater.*, 2010, **22**, 4120-4122.

4 (a) E. D. Bloch, L. J. Murray, W. L. Queen, S. Chavan, S. Maximoff, J. P. Bigi, R. Krishna, V. K. Peterson, F. Grandjean, J. Long, B. Smit, S. Bordiga, C. M. Brown and J. R. Long, *J. Am. Chem. Soc.*, 2011, **133**, 14814-14822; (b) Y. E. Cheon and M. P. Suh, *Angew. Chem., Int. Ed.*, 2009, **48**, 2899-2903.

5 (a) M. Nippe, R. S. Khnayzer, J. A. Panetier, D. Z. Zee, B. S. Olaiya, M. Head-Gordon, C. J. Chang, F. N. Gastellano, J. Long, *Chem. Sci.* 2013, **4**, 3934-3945; (b) O. R. Luca, R. H. Crabtree, *Chem. Soc. Rev.*, 2013, **42**, 1440-1459.; (c) V. K. Praneeth, M. R. Ringenberg, T. R. Ward, *Angew. Chem., Int. Ed.*, 2012, **51**, 10228-10234.

6 (a) L. Cañadillas-Delgado, O. Fabelo, J. A. Rodrínguez Velamazán, M. Lemée-Cailleau, S. A. Mason, E. Pardo, F. Llore, J. Zhao, X. Bu, V. Simonet, C. V. Colin and J. Rodríguez-Carvaj, *J. Am. Chem. Soc.*, 2012, **134**, 19772-19781; (b) A. O. Polyakov, A. H. Arkenbout, J. Baas, G. R. Blake, A. Meetsma, A. Caretta, H. M. V. Loosdrecht and T. T. M. Palstra, *Chem. Mater.*, 2012, **24**, 133-139.

7 (a) J. M. Falkowski, C. Wang, S. Liu and W. Lin, *Angew. Che Int. Ed.*, 2011, **50**, 8674-8678; (b) M. Meilikhow, K. Yusenko, A. Torrisi, B. Jee, C. Mellot-Draznieks, A. Pöppl and R. A. Fischer, *Angew. Chem., Int. Ed.*, 2010, **49**, 6212-6215; (c) C. K. Brozek and M. Dincă, *J. Am. Chem. Soc.*, 2013, **135**, 12886-12891; (d) T. Liu, L. Zou, D. Feng, Y. Chen, S. Fordham, X. Wang, Y. Liu and H. Zhou, *J. Am. Chem. Soc.*, 2014, **136**, 7813-7816; (e) J. Y. Ge, J. Wang, J. Cheng, P. Wang, J. Ma, Q. Liu and Y. Dong, *Chem. Commun.*, 2014, **50**, 4434-4437; (f) H. J .Choi and M. P. Suh, *Am. Chem. Soc.*, 2004, **126**, 15844-15851; (g) H. R. Moon, J. H. Kim and M. P. Suk, *Angew. Chem., Int. Ed.*, 2005, **44**, 1261 1265; (h) P. B. Chatterjee, A. Audhya, S. Bhattacharya, S. M. T. Abtab, K. Bhattacharya and M. Chaudhury, *J. Am. Chem. Soc*, 2010, **132**, 15842-15845.

8 J. Sun, F. Dai, W. Yuan, W. Bi, X. Zhao, W. Sun and D. Sun, *Angew. Chem., Int. Ed.*, 2011, **50**, 7061-7064.

9 (a) Y. Huang, B. Mu, P. M. Schoenecker, C. G. Carsom, J. R Karra, Y. Cai and K. S. Walton, *Angew. Chem., Int. Ed.*, 2011, **50**, 436-440; (b) Q. He, X. Li, Y. Liu, Z. Yu, W. Wang and C. Su, *Angew. Chem., Int. Ed.*, 2009, **48**, 6156-6159.

10 M. Moliner, C. Martínez and A. Corma, *Chem. Mater.*, 201, **16**, 246-258.

11 B. Balamurugan, B. R. Mehta and S. M. Shivaprasad, *App Phys. Lett.*, 2001, **79**, 3176-3178.

12 (a) F. Xu, T. Tao, K. Zhang, X. Wang, W. Huang and X. You, *Dalton Trans.*, 2013, **42**, 3631-3645; (b) S. Arai, Y. Hashimoto T. Yamagishi and M. Hida, *Bull. Chem. Soc. Jpn.*, 1989, **62**, 3143-3149.